

## Article

# Assessment of Atmospheric Correction Processors and Spectral Bands for Satellite-Derived Bathymetry Using Sentinel-2 Data in the Middle Adriatic

Ljerka Vrdoljak <sup>1,\*</sup>  and Jelena Kilić Pamuković <sup>2,\*</sup> <sup>1</sup> Hydrographic Institute of the Republic of Croatia, Zrinsko Frankopanska 161, 21000 Split, Croatia<sup>2</sup> Faculty of Civil Engineering, Architecture and Geodesy, University of Split, Matice Hrvatske 15, 21000 Split, Croatia

\* Correspondence: ljerka.vrdoljak@hhi.hr (L.V.); jelena.kilic@gradst.hr (J.K.P.)

**Abstract:** Satellite-derived bathymetry (SDB) based on multispectral satellite images (MSI) from the satellite's optical sensors is a recent technique for surveying shallow waters. Sentinel-2 satellite mission with an open access policy and high spatial, radiometric, and temporal resolution of MSI-s started a new era in the mapping of coastal bathymetry. More than 90 percent of the electromagnetic (EM) signal received by satellites is due to the atmospheric path of the EM signal. While Sentinel-2 MSI Level 1C provides top-of-atmosphere reflectance, Level 2A provides bottom-of-atmosphere reflectance. The European Space Agency applies the Sen2Cor algorithm for atmospheric correction (AC) to model the atmospheric path of the signal and reduce the MSI reflectance from L1C to L2A over the land area. This research evaluated the performance of different image-based AC processors, namely: Sen2Cor, Acolite, C2RCC, and iCOR for SDB modelling. The empirical log band ratio algorithm was applied to a time series of Sentinel-2 MSI in the middle Adriatic. All AC processors outperformed Sentinel-L2A MSI for SDB. Acolite and iCOR demonstrated accurate performance with a correlation coefficient higher than 90 percent and the RMSE under 2 m for depths up to 20 m. C2RCC produced more robust bathymetry models and was able to retrieve the depth information from more scenes than any other correction. Furthermore, a switch model combining different spectral bands improved mapping in shallow waters, demonstrating the potential of SDB technology for the effective mapping of shallow waters.

**Keywords:** bathymetry mapping; pre-processing; SNAP; switch model

**Citation:** Vrdoljak, L.; Kilić Pamuković, J. Assessment of Atmospheric Correction Processors and Spectral Bands for Satellite-Derived Bathymetry Using Sentinel-2 Data in the Middle Adriatic. *Hydrology* **2022**, *9*, 215. <https://doi.org/10.3390/hydrology9120215>

Academic Editor: Mohammad Valipour

Received: 27 September 2022

Accepted: 28 November 2022

Published: 30 November 2022

**Publisher's Note:** MDPI stays neutral with regard to jurisdictional claims in published maps and institutional affiliations.



**Copyright:** © 2022 by the authors. Licensee MDPI, Basel, Switzerland. This article is an open access article distributed under the terms and conditions of the Creative Commons Attribution (CC BY) license (<https://creativecommons.org/licenses/by/4.0/>).

## 1. Introduction

Accurate and up-to-date bathymetry is important for safe navigation [1] and underpins all activities or research on or beneath the surface of the sea [2,3]. Coastal zones, an interface between the land and the sea, are densely inhabited by approximately forty percent of the world's population living 100 km from the coast at a population density twice the global average [4]. Low-elevation coastal zones are considered the most threatened zones due to sea level rise [5,6] and extreme weather events [7] intensified with climate change. Although coastal zones are highly dynamic environments due to human and/or natural influence, more than 50 percent of the near shore bathymetry within the exclusive economic zones (EEZ) has not been mapped yet, or the bathymetry information relies on outdated surveys [8].

Classic bathymetry techniques, acoustic systems, or light detection and ranging (LiDAR), enable the bathymetry surveys with the highest quality of data [9]. Acoustic systems, e.g., the multibeam echosounder (MB) are usually mounted on research vessels with a swath width and ensonifying efficiency proportional to depth [10]. On the other hand, LiDAR is mounted on an aircraft but is limited by signal penetration to shallow waters [11]. The main limiting factor of echo sounders and LiDAR is the high cost of the survey. Compared

to traditional bathymetric techniques, remote sensing technology provides large spatial coverage with minor expenses. Satellite-derived bathymetry (SDB) based on multispectral satellite images (MSI) from the satellite's optical sensors is a recent low-cost technique for surveying shallow waters.

Sentinel-2 satellite mission with an open access policy and high spatial, radiometric, and temporal resolution of multispectral images started a new era in Earth observation (EO), including the mapping of coastal bathymetry [12]. Multispectral sensors on Sentinel-2 satellites measure the Earth's reflected radiance in 13 spectral bands. More than 90 percent of the EM signal received by the satellite is due to the atmospheric path of the EM signal [13].

The European Space Agency (ESA) uses the Sen2Cor [14] atmospheric correction (AC) processor to model the atmospheric path of the signal and reduce the reflectance from the top of the atmosphere (TOA)—Sentinel-2 Level 1C—and to the bottom of the atmosphere reflectance (BOA)—Sentinel-2 Level 2A. Both Sentinel-2 products, L1C and L2A, are distributed via the Copernicus Open Access Hub portal [15]. In addition to Sen2Cor, there are several image-based AC processors available.

Recent studies analysed the performance of different AC processors for Sentinel-2 MSI in coastal marine areas [16–19]. Casal et al. [16] selected the C2RCC among Acolite EXP, iCOR, and Sen2Cor to for best performance on the optically complex and turbid waters of Dublin Bay. An evaluation of AC processors for multitemporal SDB in low-turbid Caribbean waters was made by Caballero and Stumpf [17]. Three AC processors for Sentinel-2 MSI were evaluated: the Acolite exponential model (EXP), Acolite dark spectrum fitting model (DSF), and C2RCC model. Acolite models produced greater consistency and repeatability with accurate results in a scene-by-scene analysis. Renosh et al. [18] evaluated AC algorithms for Sentinel-2 MSI in highly turbid estuarine waters in SW France. Acolite DSF and iCOR are identified as best-performing among the tested AC algorithms (Acolite DSF, iCOR, Polymer, and C2RCC) for Sentinel 2-MSI. Duan et al. [19] combined three different AC processors (6S, Acolite, and Quac) with various SDB models and yielded acceptable results over two islands in the Pacific Ocean.

In the present study, diverse AC processors for SDB mapping have been validated along the eastern coast in the middle Adriatic. The Adriatic Sea is a shallow sea with a median depth of 100 m [20] and a highly indented eastern coast, resulting in long-lasting and costly classic bathymetric surveys. Therefore, a small part of the coastal marine area has been mapped in high resolution using modern acoustic technology [21,22]. The optical characteristics of the sea in the middle Adriatic make the region suitable for SDB [23,24]. SDB mapping of the Adriatic has demonstrated that the technology can retrieve depth with a horizontal accuracy of 12.5 m [25], a vertical accuracy of 2 m + 5% depth [25], and a spatial resolution of up to 10 m.

The scope of this paper was to determine whether the quality of SDB could be improved by applying one of the available AC processors to Sentinel-2 L1C rather than using Sentinel-2 L2A. In addition to Sentinel-2 L2A MSI, three other AC processors have been selected: atmospheric correction for the OLI 'lite' (Acolite) [26–29], Case 2 Regional Coast Colour (C2RCC) [30,31], and image correction for atmospheric effects (iCOR) [32,33]. All these AC processors are image-based ACs and free for users. In the absence of reflectance measured in situ, the bathymetry retrieved by each processor is validated using in situ soundings.

In shallow water areas, spectral bands with a wavelength from 380 nm to 700 nm known as visible light (VIS) can reach the seafloor. The empirical approach and the simple log band ratio (LBR) algorithm [34] are widely adapted for SDB depth estimation [35–38]. The LBR algorithm uses the ratio of two bands to estimate bathymetry. Recent studies demonstrated that bands with long wavelengths are less influenced by sediment dynamics and water turbidity, therefore possessing better performance in SDB retrieval in the shallowest coastal sea area than short wavelengths [39–41]. Four bands in the VIS part of the spectrum of the Sentinel-2 MSI can retrieve bathymetry: band 1—coastal aerosol,

band 2—blue, band 3—green, and band 4—red. The second objective of the study was to combine bands using the LBR algorithm in combinations different from the common one of blue and green bands [34], with the scope to achieve an enhanced bathymetric model.

## 2. Methods and Methodology

The methodology has been divided into two sections, related to the AC of Sentinel-2 L1C MSIs, and the switch model. The influence of the atmosphere and water on the observed radiance at the satellite, key information regarding the AC processors, and the basic principle of the LBR algorithm are considered in the first part. Further on, a switch model as an enhancement of LBR is introduced in the second part.

### 2.1. Remote Sensing of Shallow Marine Areas

Optical sensors mounted on satellites (e.g., the multispectral instrument onboard Sentinel-2 satellites) are passive systems that record a reflected radiance coming from the Sun. From Sun to satellite, the EM signal passes a two-way path. First, a downwelling radiance from the Sun must reach the seafloor, and then an upwelling radiance has to reach the sensor. The signal interacts with the atmosphere, sea surface, waterbody, and seafloor, which includes attenuation, scattering, and reflection of the signal. The spectral radiance at the top of the atmosphere that is measured from a satellite ( $L_T$ ) consists of the radiance scattered in the atmosphere and surrounding land area ( $L_P$ ), radiance reflected from the sea surface ( $L_S$ ), radiance backscattered by constituents present in seawater and in very shallow water reflected by the seafloor ( $L_B$ ) [13]:

$$L_T = L_P + L_S + L_V + L_B \quad (1)$$

To retrieve the radiance reflected by the seafloor, a correction for the atmospheric path of the signal and surface reflections must be calculated. Clouds are the main cause of signal reflection in the atmosphere [42]; therefore, MSI with a high percentage of clouds should be avoided. The scattering of the EM signal by air gas molecules known as Rayleigh scattering and Mie scattering by larger particles of aerosol [43] can be eliminated by the AC processor.

A part of the received signal is a result of the reflection from the sea surface or adjacent areas. Specific, direct specular reflection of the EM signal that occurs when the reflection angle equals the viewing angle is called the sunglint [44]. Scattering due to dissolved particles in the seawater (turbidity) is also a contributor to the radiance received by satellites.

The heterogeneity of seafloor type (albedo) is usually not covered by the AC processor. However, their influence can be minimized by the choice of the SDB method to estimate depth.

### 2.2. Atmospheric Correction

Atmospheric correction (AC) eliminates part of the reflectance that refers to the atmospheric path of the electromagnetic (EM) signal received by satellite. Atmospheric scattering is estimated to account for more than 90% of the total measured radiation [13]. It is the process of converting radiation received by the satellite sensor to surface reflectance [45].

Sen2Cor is an AC processor that performs atmospheric correction of top-of-atmosphere (TOA) Sentinel-2 Level 1C input scenes and generates bottom-of-atmosphere (BOA) Sentinel-2 Level 2A-corrected reflectance scenes. It is available as a plugin through the Sentinel Application Platform (SNAP) or as a standalone application [15]. Telespazio VEGA Deutschland GmbH developed the processor on behalf of ESA [46]. It is an adaptation of ATCOR software [47] that derives aerosol optical thickness (AOT) from the look-up tables (LUT) at 550 nm using the dense dark vegetation (DDV) algorithm [48]. The algorithm requires that the scene contains sufficiently dark pixels for which it can be assumed that the BOA reflectance of different bands is constant. If pixels containing DDV are not present in a scene, they can be replaced by pixels of dark soil or water. The algorithm automatically chooses these pixels, derived from the AOT, and corrects the image. It does not correct for

sunglint effects. ESA processes the Sentinel-2 L1C products with the Sen2Cor algorithm to distribute the Sentinel-2 L2A products.

Apart from Sen2Cor, there are different AC processors to choose from. This research evaluated the performance of Sentinel-2 Correction (Sen2Cor), atmospheric correction for OLI ‘lite’ (Acolite), Case 2 Regional Coast Colour (C2RCC) and image correction for atmospheric effects (iCOR) for bathymetry estimation. All AC processors are image-based ACs that do not require additional atmospheric measurements. However, they differ in technique when modelling the variable contribution of scattering from aerosols and the ability to eliminate undesirable surface reflections (e.g., sunglint or adjacent area). Further on, a key distinguishing characteristic of each AC processor is briefly addressed with references to the key research containing mathematical models and more detailed descriptions. In Table 1, the main properties of each correction are presented.

**Table 1.** Characteristics of AC processors: atmospheric scattering model, elimination of surface reflection, and key references providing a more detailed description of each AC [14,26–33,47,48].

AC	Sen2Cor	Acolite EXP	Acolite DSF	iCOR	C2RCC
Intended for:	Sentinel-2 MSI over land	Sentinel-2 and Landsat MSI over turbid waters	Metre-resolution MSI for aquatic application	Inland, coastal or transitional waters and land	All past and current ocean sensors over normal and extreme optically complex waters
AOT—retrieval algorithm	Dark dense vegetation algorithm	Extrapolation from SWIR to VIS and IR using an exponential function	Automatic selection of band with the lowest estimate of atmospheric path reflectance	Adaptation of Self-Contained Atmospheric Parameters Estimation from Meris data (SCAPE -M) method	Trained neural network and coastal aerosol model
Adjacency effect	-	-	-	SIMEC module	-
Sunglint	-	-	Yes	-	Yes
Turbidity	-	-	-	-	5-component bio-optical model
References	[14,47,48]	[26,27]	[28,29]	[32,33]	[30,31]

Acolite is an AC processor developed at the Royal Belgian Institute of Natural Sciences that supports many sensors including one from the Sentinel-2 mission. It is available as a stand-alone installation [49]. Two AC approaches are included: “exponential extrapolation (EXP)” [26,27] and “dark spectrum fitting (DSF)” [28,29].

Acolite EXP was developed as the AC processor for Landsat and Sentinel images over turbid waters. The algorithm assumes that the reflectance in the SWIR bands contains only information about aerosol and Rayleigh scattering due to the high absorption coefficient in water. After the signal is corrected for the Rayleigh scattering it is extrapolated from the SWIR band to visible light (VIS) and infrared (IR) using an exponential function. Due to the sun glint and adjacency effect, the performance of the Acolite EXP was not satisfactory in low turbidity waters, often resulting in negative reflectance [29]. The performance of the EXP processor regarding Sentinel-2 scenes was also degraded in the blue bands by a higher signal-to-noise (S/N) ratio [50]. Acolite dark spectrum fitting (DSF) overcomes the issues of the EXP method by automatic selection of the most appropriate band with the lowest atmospheric path reflection and further estimation of AOT based on look-up tables (LUT). It was developed for high-resolution satellite images (meter-scale) but can be applied to Sentinel-2 scenes due to better spectral resolution in the SWIR band. It provides the estimation of a sun glint reflectance using the SWIR band [29]. Both Acolite algorithms mask the land area and negative reflectance.

The Case 2 Regional processor is based on a neural network trained by a large database of radiative transfer simulations of water leaving radiance (“water signal”) and related TOA radiance (“satellite signal”) [30]. Neural networks are used for the inversion of satellite and

water signal. A major improvement was made through the CoastColour project when the 5-component bio-optical model and coastal aerosol model were introduced. The in-water modelling is performed by the Hydrolight model, using 5 components as an abstract of inherent optical properties (IOP) in natural waters. The processor was renamed to Case 2 Regional Coast Colour (C2RCC) and is available through the SNAP platform [31]. C2RCC is designed for turbid waters. It includes sun glint correction and the automatic creation of the land mask.

Image correction for atmospheric effects (iCOR) is the latest version of the Operational Atmospheric Correction for Land and Water (OPERA) AC processor designed for inland, coastal, or transitional waters and land [32]. Key steps in the AC algorithm are the separation of land and water pixels, deriving AOT using land pixels [51], and applying the SIMEC [33] correction over water. AOT retrieval algorithm used in iCOR is an adaptation of Self-Contained Atmospheric Parameters Estimation from Meris data (SCAPE-M) [51]. SIMEC reduces the contamination of the water pixels by the light coming from the surrounding land and vegetation. The next step is solving the radiative transfer equation using the MODTRAN5 LUT to perform the AC. The current version does not support the sun glint correction.

The selected Sentinel-2 L1C MSIs were processed by the different AC processors listed above. A few changes were made to the default settings of the AC processors. Combination of B8A—Vegetation red edge ( $\lambda_i = 865$  nm) and B11 SWIR—Short-wave infrared ( $\lambda_j = 1610$  nm) was chosen for the Acolite EXP algorithm. Recent studies demonstrated this combination reduces the influence of the NIR/SWIR instrument noise [17]. An extra iCOR module SIMEC was enabled. For all AC processors other than ACOLITE and C2RCC, the land mask was determined from the near-infrared (NIR) band [52]. Remote sensing reflectance ( $R_{rs}$ ) was calculated for all scenes and AC processors. A median filter was applied to all scenes to reduce the noise in the model [17].

In the absence of in situ measured reflectance, the evaluation of the AC processor performance in retrieving the bathymetry information was conducted in comparison with in situ measured depth [16,17].

### 2.3. Log Band Ratio Algorithm

The concept underlying the log ratio algorithm is that the radiance of one band decays faster in depth than that of another band [34]. Beer's law states that the absorbance of the EM signal is directly proportional to the length of the path and absorption coefficient of the spectral band ( $K_\lambda$ ). Accordingly, the ratio of the two bands changes with depth.

Bathymetry for each scene was estimated by the log band ratio (LBR) algorithm [34]:

$$\text{pSDB} = \frac{\ln(nR_w(\lambda_i))}{\ln(nR_w(\lambda_j))} \quad (2)$$

where pSDB refers to the relative pseudo-depth model,  $n$  is the constant to avoid a negative algorithm,  $R_w$  is the water leaving reflectance, and  $\lambda_i$  and  $\lambda_j$  are two different bands [17,34]. SDB is determined by regression analyses between the pseudo-depth and the MB control soundings [17,34]:

$$\text{SDB} = m_1 \text{pSDB} - m_0 \quad (3)$$

where  $m_1$  and  $m_0$  are the empirically determined gain and offset of the regression line. The method is proven effective for clear, shallow water bathymetry mapping, with only two coefficients to be empirically determined. It can be applied in areas with little a priori known bathymetry data. The method is not sensitive to the change of bottom type since both spectral bands are equally influenced. The band ratio is more affected by the depth change due to the different absorption coefficients of bands [34].

Classic green LBR, the ratio of Sentinel-2 band 2—blue ( $\lambda_i = 490$  nm) and Band 3—green ( $\lambda_j = 560$  nm), was used for the estimation of bathymetry [34]. Products of the LBR algorithm (pSDB and SDB) for each scene were compared to soundings from the

multibeam survey. The consistency and accuracy of retrieving depth was evaluated for each AC algorithm.

#### 2.4. Switch Model

The LBR algorithm [34] is the basis of the switch bathymetry model [40]. In shallow seas, visible light (380–700 nm) is a segment of the EM spectrum that can reach the sea bottom and retrieve bathymetric information. Sentinel-2 satellites collect four spectral bands in the VIS part of the EM spectrum: B1—coastal Aerosol (blue part of VIS), B2—blue, B3—green, and B4—red. Blue and green spectral bands have a smaller coefficient of absorption in water than the red spectral band (Figure 1).

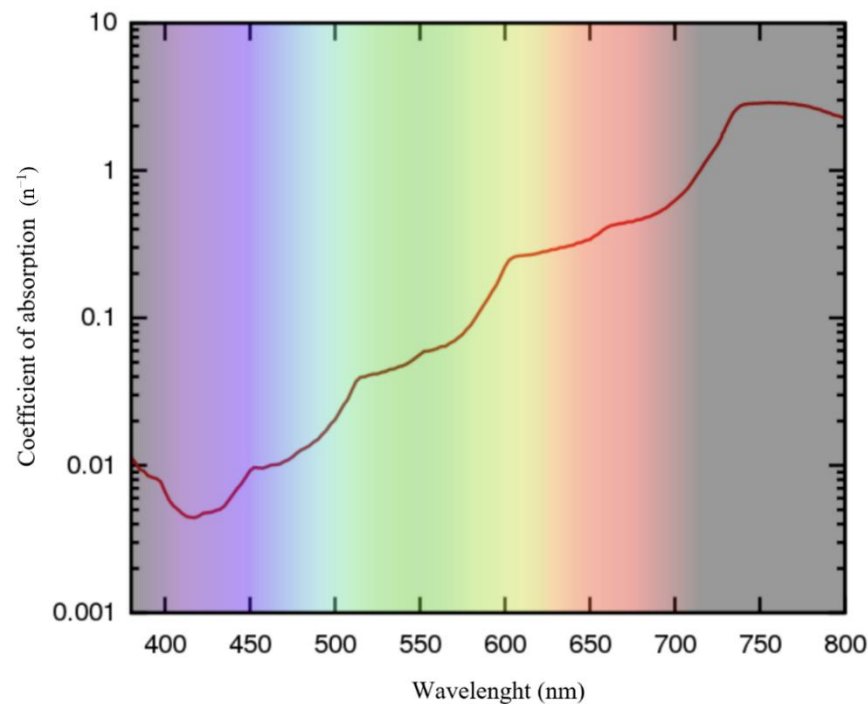


**Figure 1.** Absorption coefficient of VIS in water [53].

Accordingly, a blue or a green signal decays more slowly while traveling through the water column. This paper explored the possibility of enhancing the bathymetry model in the coastal zone by augmenting the bathymetry estimated using the classic green (G) LBR with the bathymetry estimated using a red LBR algorithm. The red (R) LBR applied the red band (B4) instead of the green one (B3) (Table 2). Sentinel-2 band 1—coastal aerosol, which belongs to the blue part of VIS, was overlooked because of the lower spatial resolution and greater S/N ratio.

**Table 2.** Band combinations applied in the LBR algorithm.

	Band	$\lambda$ [nm]
G	B2 blue	490
	B3 green	560
R	B2 blue	490
	B4 red	665

The switch model was calculated by applying the weighted mean between the G SDB and R SDB [40]:

$$\text{Switch SDB} = \alpha \times G + \beta \times R, \quad (4)$$

$$\alpha + \beta = 1, \quad (5)$$

where coefficients ( $\alpha$ ,  $\beta$ ) were empirically determined.

### 3. Results

Results of the assessment of AC processors for SDB retrieval and the switch model from Sentinel-2 MSI in the middle Adriatic, following the methodology described above, are presented in the following chapter.

#### 3.1. Study Area

Research of optical characteristics in the coastal area of the middle Adriatic far from river mouths, etc., characterized water type to be equivalent to oceanic water type II, according to Jerlov classification [23]. The Šibenik channel, located in the middle Adriatic near the city of Šibenik was chosen as a location for the study area (Figure 1). The location is suitable for the comparison and evaluation of the AC processors because of uniform water conditions throughout the year and the availability of high-resolution, up-to-date survey data. According to bathymetry, the channel can be divided into three sections: shallow eastern and western parts with depths up to 30 m, separated by the deeper channel with depths up to 60 m that follow from the Saint Antoine's channel. The topography of the seafloor shows a dynamic gradient of depth with many shoals, especially in the east. The seafloor is mostly covered with sand [54].

Evaluation of the depth retrieval performance of different AC processors was conducted in the west part of the Šibenik channel and the switch digital bathymetry model was calculated for the broader area (Figure 2).

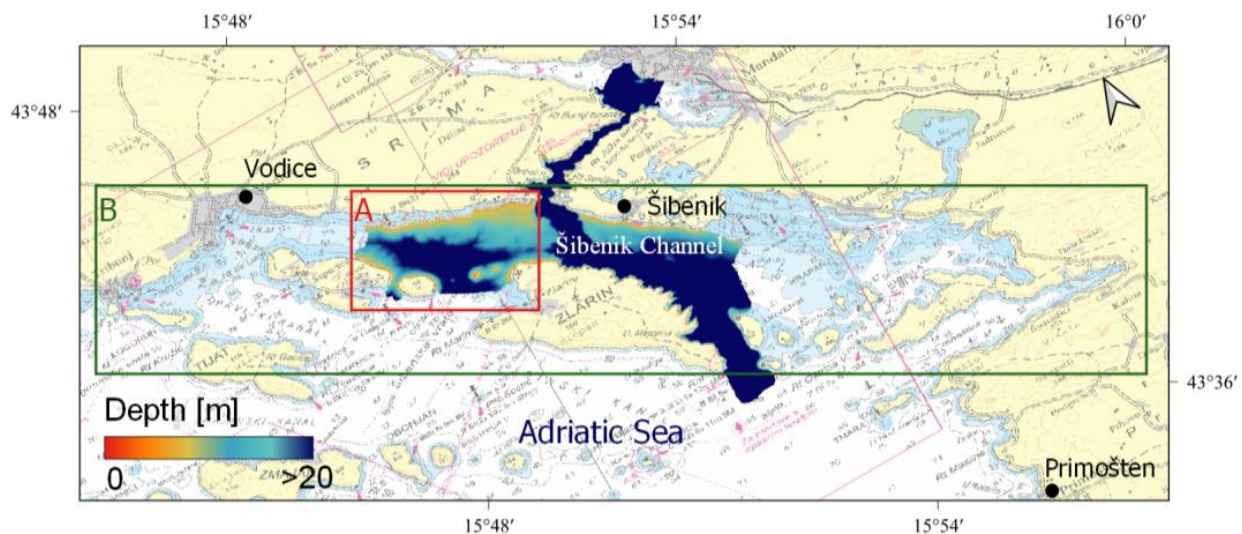


**Figure 2.** The study area and the MB survey. The red rectangle defines area: A for the evaluation of the AC processors and the green rectangle defines broader area; B for bathymetry estimation.

#### 3.2. Dataset

The empirical SDB approach requires the MSI data and a priori known soundings for bathymetry estimation. A time series of Sentinel-2 MSI covering a year was selected for the study area in the Šibenik channel (middle Adriatic) where a recent MB survey was conducted.

##### 3.2.1. Multibeam Bathymetry Data

The Hydrographic Institute of the Republic of Croatia (HHI) surveyed the area of Šibenik's channel, Saint Antoine's channel, and Šibenik's port in 2014 to ensure the safety of navigation in the area (Figure 2) [21]. Dual head multibeam echosounder Kongsberg

EM-3002 D swiped the seafloor with quality of depth defined by special order of the S-44 standard, including total horizontal uncertainty (THU) under 2 m and total vertical uncertainty according to Formula [9]:

$$TVU = \sqrt{a^2 + (b \times d)^2} \quad (6)$$

where  $a = 0.25$  m,  $b = 0.0075$ , and  $d$  is depth. Survey data was post-processed in Seafloor Information System (SIS) software and reduced to mean low lower water (MLLW). Data were interpolated to a bathymetry model (MB DBM) with 10 m grid spacing in WGS84/UTM 33 coordinate system. MB bathymetry data ranging between 0 and 20 m were randomly chosen as control or check soundings. Of the available soundings within test area A or B, 25% were chosen as MB control data ( $N_{\text{control}}^A = 9141$ ,  $N_{\text{control}}^B = 16,890$ ) and 75% as the MB check data ( $N_{\text{check}}^A = 27,423$ ,  $N_{\text{check}}^B = 50,670$ ) (Figure 2). Control data were necessary for the vertical calibration of the SDB. Check data were used for quality control.

### 3.2.2. Sentinel-2 Multispectral Images

The Sentinel-2 satellite mission started a new area in coastal bathymetry mapping with an open-access policy, high-resolution images, and a 5-day revisit time. Two twin satellites (Sentinel-2A and Sentinel-2B), placed in the same sun-synchronous orbit and phased at 180° to each other, carry a multispectral instrument that samples 13 spectral bands [55] (Table 3).

**Table 3.** Sentinel-2 band list. Spectral bands able to reach the seafloor (Visible light VIS) are bolded [55].

Band	Spectral Region	Centre Wavelength/Band Width [nm]		Spatial Resolution [m]
		S2A	S2B	
<b>B1</b>	<b>Coastal Aerosol (CB)</b>	<b>442.7/21</b>	<b>442.2/21</b>	<b>60</b>
<b>B2</b>	<b>Blue (B)</b>	<b>492.4/66</b>	<b>492.1/66</b>	<b>10</b>
<b>B3</b>	<b>Green (G)</b>	<b>559.8/36</b>	<b>559.0/36</b>	<b>10</b>
<b>B4</b>	<b>Red(R)</b>	<b>664.6/31</b>	<b>664.9/31</b>	<b>10</b>
B5	Red edge 1	704.1/15	703.8/16	20
B6	Red edge 2	740.5/15	739.1/15	20
B7	Red edge	782.8/20	779.7/20	20
B8	Near-infrared (NIR)	832.8/106	832.9/106	10
B8A	Near-infrared narrow (NIR)	864.7/21	864.0/22	20
B9	Water vapour	945.1/20	943.2/21	60
B10	Shortwave infrared/cirrus	1373.5/31	1376.9/30	60
B11	Shortwave infrared 1(SWIR1)	1613.7/91	1610.4/94	20
B12	Shortwave infrared 2(SWIR2)	2202.4/175	2185.7/185	20

The Copernicus Open Access Hub provides Sentinel-2 MSIs as two products: Level 1C, top-of-atmosphere (TOA) reflectance, and Level 2A bottom-of-atmosphere (BOA) reflectance [56]. Sentinel-2 MSI (L1C and L2A) that were collected throughout 2017 and 2018 were downloaded for the study area via the Copernicus Open Access Hub. The limit value of the cloud filter was set to 10 percent and scenes were chosen to cover each month of the year (Table 4).

### 3.3. Atmospheric Correction

The performance of different AC processors, namely Acolite DSF, Acolite EXP, C2RCC, iCOR, and Sen2Cor for bathymetry retrieval from Sentinel-2 MSI was evaluated through a comparison with soundings from the MB survey. The study area, located in the Šibenik channel (middle Adriatic) is a low-turbidity, micro-tidal area with small annual variations of the sea column suitable for the evaluation of different AC algorithms.

Twelve Sentinel-2 scenes, Level 1C (top-of-atmosphere reflectance—TOA) collected through 2017 and 2018 were processed with different AC processors. After AC algorithms were applied, several scenes were masked out due to sun glint or adjacency effects: five

MSI (1, 2, 6, 8, 11) by Sen2Cor algorithm, three MSI (5, 6, 11) by Acolite EXP, three MSI (8, 9, 12) by iCOR algorithm and two MSI (5, 6) by Acolite DSF (Table 5).

**Table 4.** List of Sentinel-2 MSI chosen for the Šibenik Channel.

No.	Satellite	Date	Time [UTC]	Azimuth (Sun)	Zenith (Sun)	Cloud %	MLLW [m]
1	2A	9 March 2017	9:50	157.39	50.57	1.21	0.08
2	2A	29 March 2017	9:50	156.23	42.61	0.00	0.10
3	2A	18 May 2017	9:50	150.13	26.73	0.14	−0.17
4	2A	28 May 2017	9:50	147.98	25.08	2.42	0.03
5	2B	12 July 2017	9:50	143.48	25.59	0.06	0.14
6	2A	6 August 2017	9:50	148.27	30.42	0.04	0.20
7	2B	30 September 2017	9:30	163.47	47.98	0.00	−0.23
8	2A	15 October 2017	9:50	166.27	53.38	0.01	−0.16
9	2A	04 November 2017	9:52	168.23	60.03	0.00	0.07
10	2B	19 December 2017	9:54	166.18	68.39	0.43	0.00
11	2B	18 January 2018	9:53	162.28	66.20	0.03	−0.04
12	2B	27 February 2018	9:50	158.09	54.51	6.68	0.18

**Table 5.** The correlation between pSDB calculated by classic green LBR [16] using Sentinel-2 MSI and control MB soundings.

AC	MSI L2A Sen2Cor	Acolite DSF	Acolite EXP	C2RCC	iCOR
MSI	$r_p$ [%]	$r_p$ [%]	$r_p$ [%]	$r_p$ [%]	$r_p$ [%]
1	-	90.35	91.40	85.42	91.35
2	-	93.66	94.41	90.23	91.64
3	<b>80.41</b>	<b>93.02</b>	<b>86.31</b>	<b>86.29</b>	<b>95.04</b>
4	<b>84.18</b>	<b>91.35</b>	<b>88.11</b>	<b>74.10</b>	<b>92.25</b>
5	87.55	-	-	79.00	92.98
6	-	-	-	66.77	90.67
7	<b>94.03</b>	<b>93.94</b>	<b>95.22</b>	<b>79.99</b>	<b>94.98</b>
8	-	92.53	92.89	84.52	-
9	83.29	91.53	88.44	81.17	-
10	<b>86.49</b>	<b>86.93</b>	<b>85.91</b>	<b>80.02</b>	<b>86.66</b>
11	-	91.72	-	80.01	91.01
12	86.48	90.35	89.09	81.75	-
N	7	10	9	12	9
Mean <sub>1</sub> $r_p$ [%]	86.06	91.54	90.20	80.77	91.84
Mean <sub>2</sub> $r_p$ [%]	<b>86.28</b>	<b>91.31</b>	<b>88.89</b>	<b>80.10</b>	<b>92.23</b>

The AC algorithms showed different results among the scenes in the study area. In terms of the correlation between the pseudo-depth (pSDB) and control MB soundings, it was possible to classify them into two groups: in the first group ACOLITE DSF, ACOLITE EXP, and iCOR showed quite good performance with a mean correlation coefficient of all scenes larger than 0.90, and in the second group C2RCC and Sen2Cor achieved weaker correlation (Table 5).

SDB was compared to check MB data for quality control. Regarding the statistics of residuals, AC processors iCOR, Acolite DSF, and Acolite EXP had comparable performances with the lowest value of root mean square error (RMSE) between scenes and median absolute error (MedAE) of 1.00 m, 1.08 m, and 1.15 m. Sen2Cor and C2RCC also had similar but less accurate performances with ( $\cong 25\%$ ) higher RMSE and MedAE of 1.63 m and 1.65 m (Table 6).

**Table 6.** Quality statistics (RMSE and absolute error (AE)) for SDB processed with different AC processors: Sen2Cor (Sentinel-2 L2A, Acolite DSF, Acolite EXP, C2RCC, iCOR).

AC	MSI L2A Sen2Cor	Acolite DSF	Acolite EXP	C2RCC	iCOR
Min RMSE [m]	1.76	1.72	1.53	1.98	1.50
Max RMSE [m]	2.67	2.54	2.54	3.74	2.46
Mean RMSE [m]	2.40	2.02	2.10	2.61	1.91
Mean AE [m]	1.92	1.51	1.58	2.03	1.39
Median AE [m]	1.65	1.08	1.15	1.63	1.00

To demonstrate the practical use of AC processors, a Sentinel-2 MSI collected on 30 September 2017 was selected as an optimal scene. The performance of the AC processors: Acolite DSF, Acolite EXP, C2RCC, iCOR, and Sen2Cor was demonstrated using the B2 band—blue. As presented in Figure 3, different processors yielded diverse results on a smaller test area, adjacent to the coast but covering only the sea. Rrs shows different values due to different methods utilized by each AC processor (see Table 1) to model the atmospheric scattering and the possibility to eliminate surface reflection or turbidity. Rrs could not be validated due to the absence of in situ measured water-leaving reflectance. However, as the focus of this paper is the assessment of different AC processors for SDB from Sentinel-2 data in the middle Adriatic, we have validated the AC processors by comparing the estimated SDB models with in situ MB check soundings.

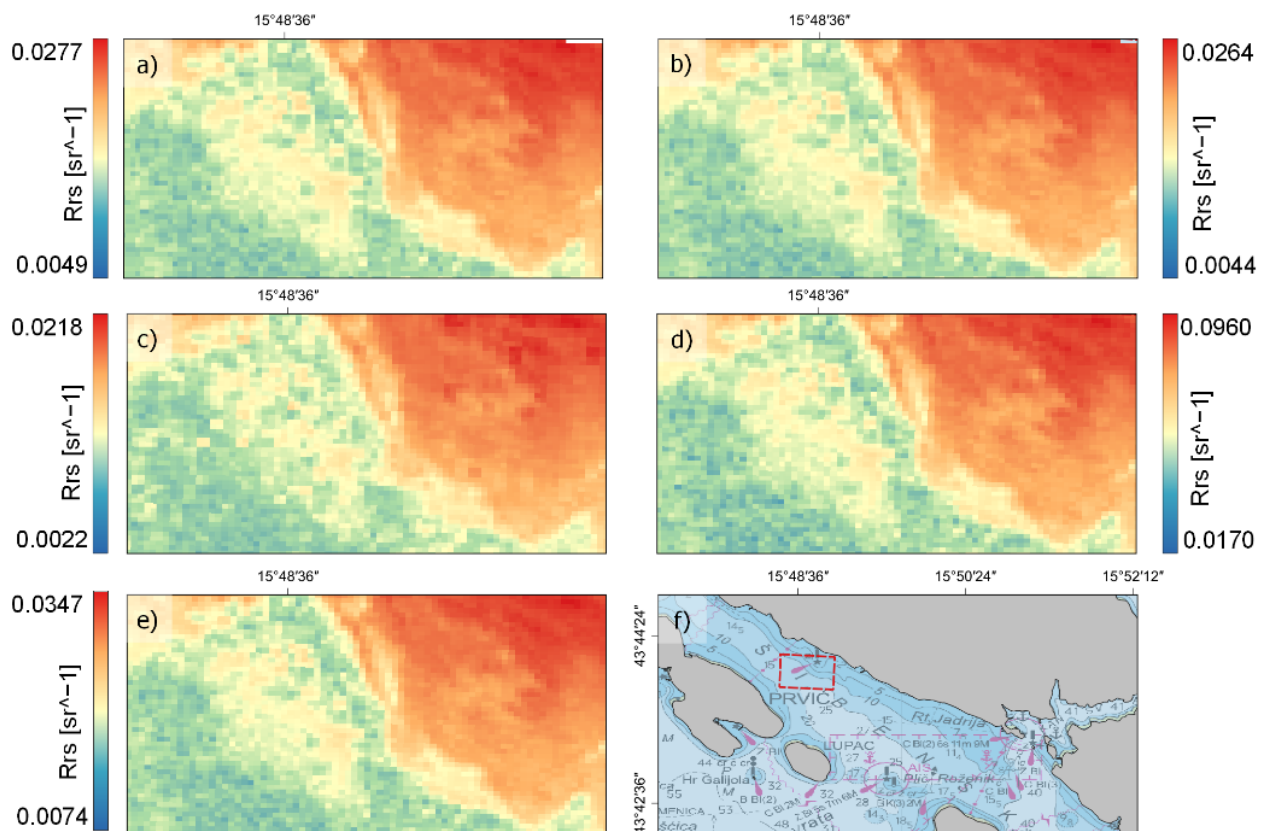


**Figure 3.** The performance of AC processors is demonstrated on a smaller marine area (f). Blue band (B2) from the optimal scene collected on 30 September 2017 was processed with different AC algorithms and remote sensing reflectance was calculated for: (a) Acolite DSF, (b) Acolite EXP, (c) C2RCC, (d) iCOR, and (e) Sen2Cor (Sentinel-2 L2A).

All AC algorithms applied to the optimal scene achieved a strong linear relationship between a pseudo-depth and control MB soundings with coefficients of determination ( $R^2$ ) larger than 80%. SDB models with depths up to 20 m, estimated by the G LBR algorithm from the optimal scene processed by different AC algorithms, are presented in Figure 4.

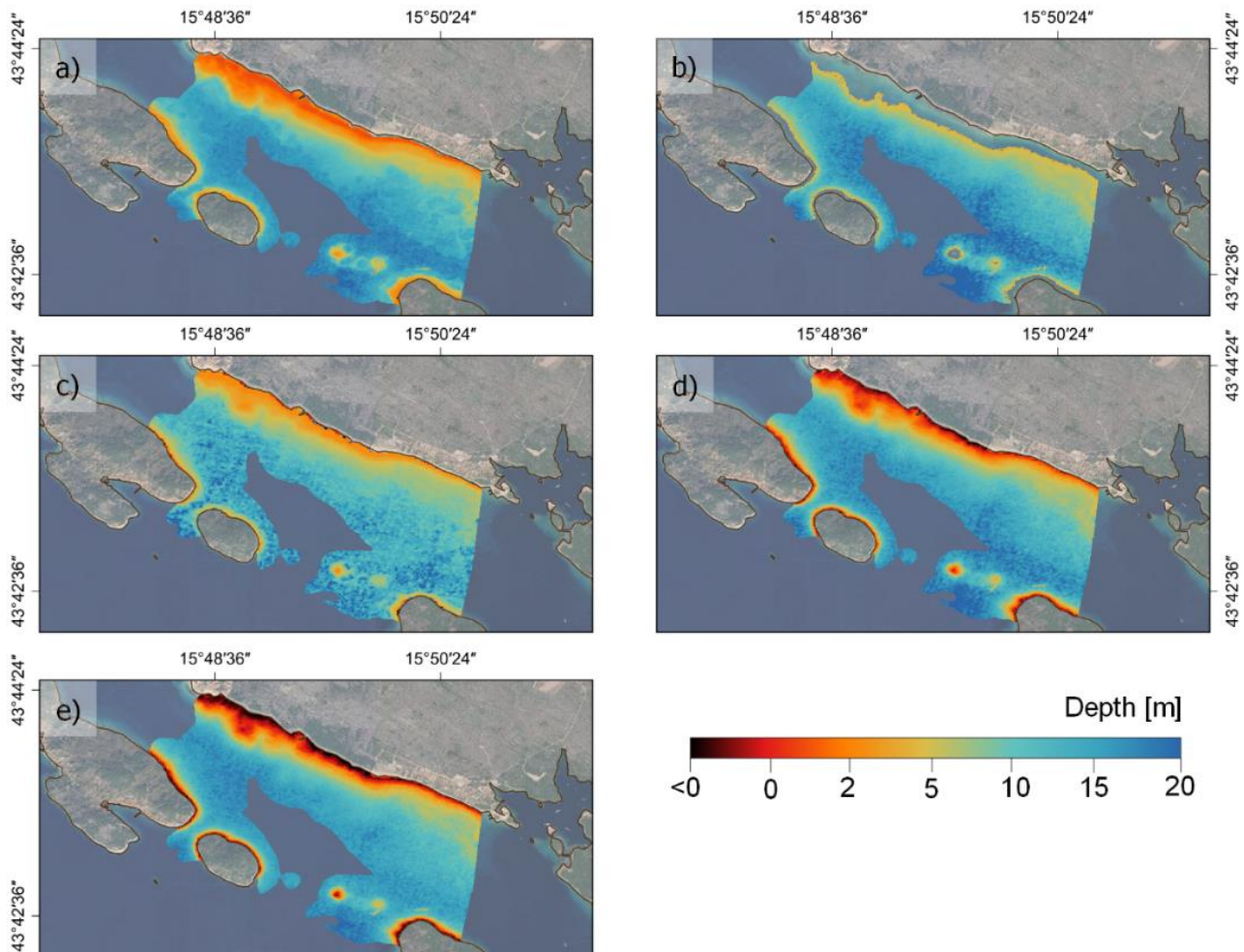


**Figure 4.** Bathymetry of the study area in the Šibenik channel (middle Adriatic) estimated from the optimal scene collected on 30 September 2017 and pre-processed with different AC algorithms: (a) Acolite DSF, (b) Acolite EXP, (c) C2RCC, (d) iCOR, and (e) Sen2Cor (Sentinel-2 L2A).

Generally, the smallest deviation from a one-to-one line and the highest correlation between the estimated depth (SDB) and check MB soundings were in the depth range between 5 m and 15 m (Figure 5). The plot shows a satisfactory adjustment of predicted depth to a one-to-one line for the Acolite DSF processor. ACOLITE EXP masked the coastal areas shallower than 5 m (Figures 4 and 5). Overestimation of depth in areas shallower than 7 m and underestimation in areas deeper than 20 m were depicted for the C2RCC algorithm as the bulk of the data was over or under the one-to-one line. Depths predicted from an MSI processed by iCOR showed adequate alignment to the one-to-one line with a slight underestimation of depth in certain ranges: shallower than 3 m and deeper than 15 m. Scatter plots of the MB survey against the SDB digital bathymetry models (DBM) derived from optimal image and processed by the Sen2Cor algorithm had a poor agreement to the one-to-one line, with the bulk of depth under the one-to-one line in depth range under 4 m and over 15 m depth and overestimation of depth in areas from 4 to 15 m deep. As can be seen in Figure 4, underestimation of depth, resulting from iCOR and Sen2Cor AC processors, resulted in negative depth in the coastal areas.

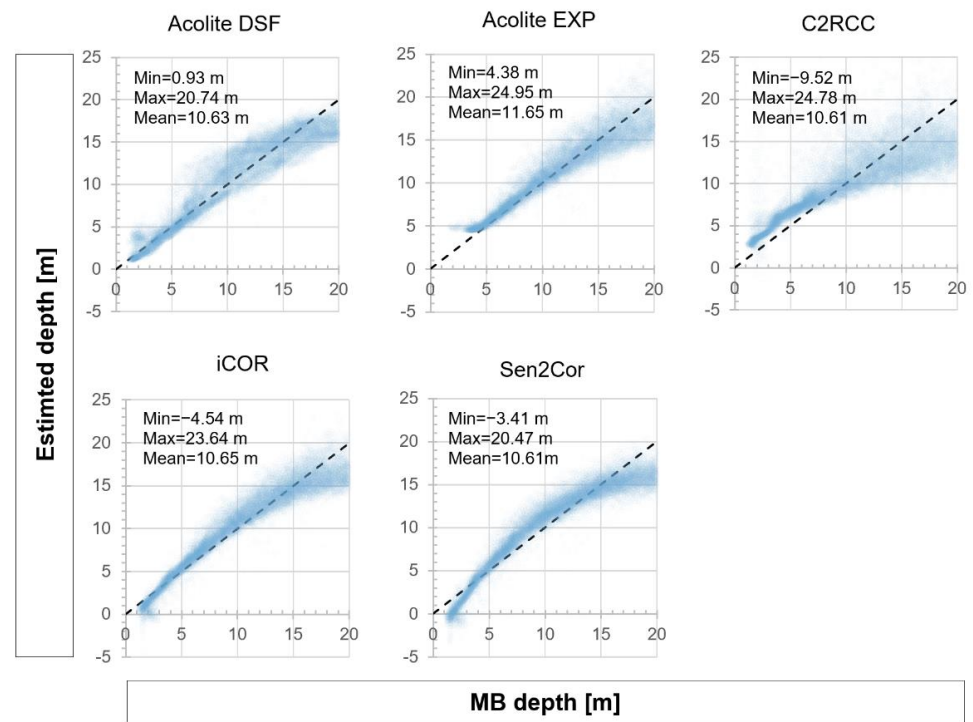


**Figure 5.** Dispersion of residuals between the estimated depth (SDB) and check MB soundings for the optimal Sentinel-2 scene (30 September 2017) pre-processed with different AC processors.

All the AC processors were efficient in retrieving depth using an optimal MSI with the RMSE under 2 m, and small MedAE up to 1.09 m with residuals grouped around zero (Figure 6).

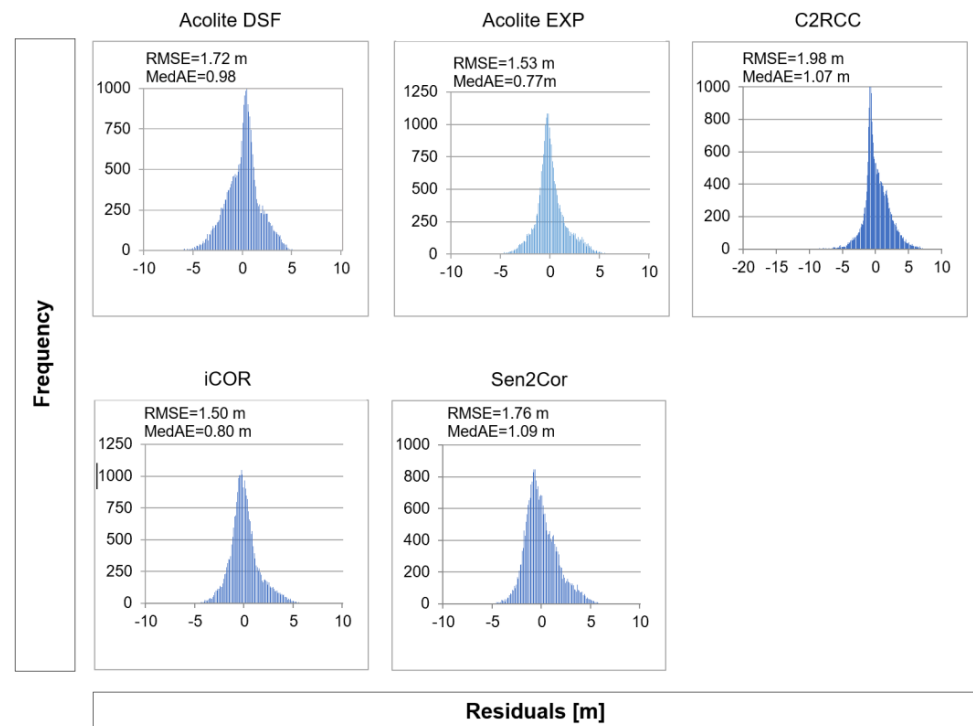


**Figure 6.** Histogram of residuals between the estimated depth (SDB) and check MB soundings for the optimal Sentinel-2 scene (30 September 2017) pre-processed with different AC processors.

Figure 7 presents the distribution of the normalized median absolute error (NMedAE) of SDB for different AC processors in various depth ranges. Inside a depth range from 5 to 20 m, all AC processors have a low value of NMedAE (under 20% of the median depth in the range). However, regardless of the AC processor, the green LBR showed poor performance in the shallowest marine area. Especially in areas shallower than 3 m, where Acolite EXP and C2RCC had NMedAE higher than 100%.

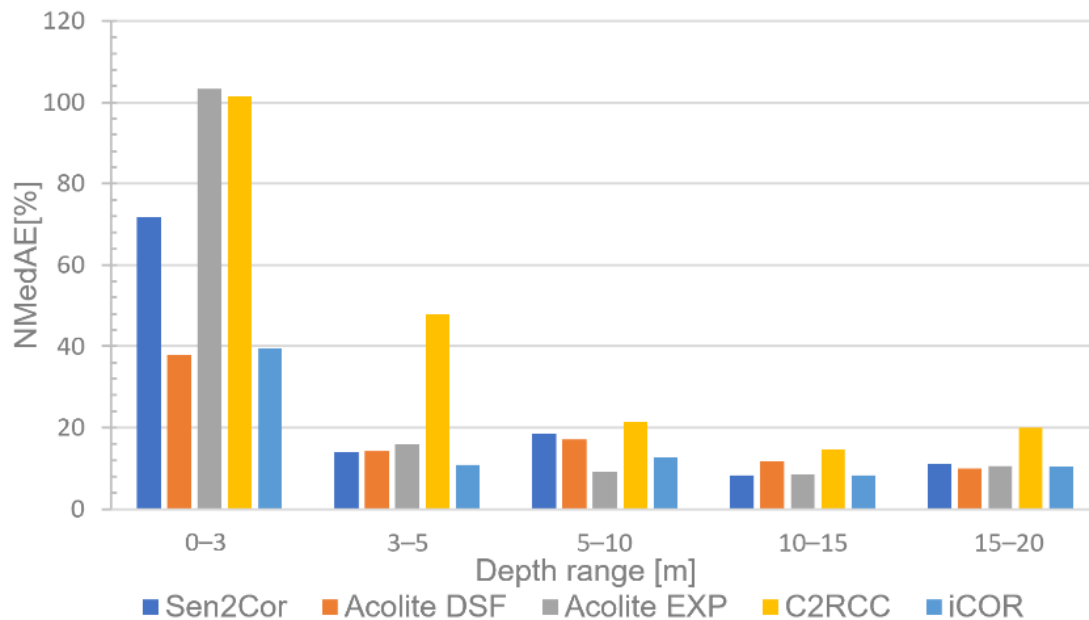


**Figure 7.** The median absolute error of the SDB estimated from the optimal scene (30 September 2017) pre-processed with different AC processors in depth ranges: 0–3 m, 3–5 m, 5–10 m, 10–15 m, 15–20 m.

### 3.4. Switch Model

Sentinel-2 satellites collect four spectral bands in the visible light (VIS) part of the EM spectrum (Table 3). As compared to Sentinel-2 red spectral band (B4), blue (B1 and B2) and green (B3) spectral bands have a smaller coefficient of absorption in water, so the extinction depth (or optical depth limit) should theoretically be deeper for the green and blue band. The optimal image acquired on the 30 September 2017 was pre-processed by the Acolite DSF algorithm. The median filter was applied to reduce the noise. The land area was automatically masked by the Acolite DSF AC processor. In the study area of the Šibenik channel, the extinction depth of VIS spectral bands was determined empirically by comparing the reflectance value of the band and the corresponding depth along a line from the coast to the deep sea.

The extinction depth for the blue (B1 and B2) and green (B3) bands was 20 m and for the red (B4) band was 5 m (Figure 8). Band B1—coastal aerosol—was excluded from further calculation due to smaller spatial resolution and higher signal-to-noise ratio. Two combinations of spectral bands for the LBR algorithm were defined: classic green (G) LBR (ln blue/ln green), and red (R) LBR (ln blue/ln red). Both versions of LBR algorithms, green and red, achieved a high correlation between pseudo-depth models and control MB soundings. R LBR had higher dispersion around the regression line (Figure 9).

Accuracy assessment of G SDB and R SDB was conducted by comparing them with the check MB soundings. The RMSE of SDB models demonstrated the strong performance of the LBR algorithm for both combinations (RMSE  $\cong$  10% depth range) (Table 7).

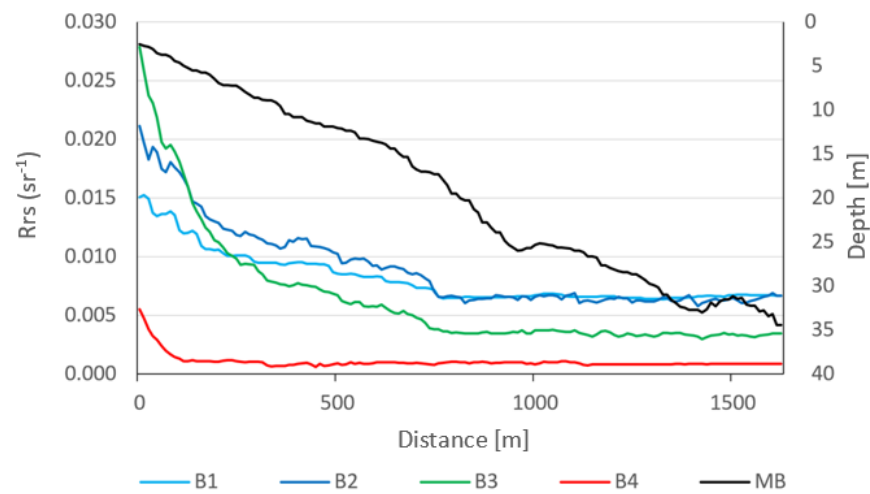


**Figure 8.** Extinction depth of VIS bands for the Sentinel-2 MSI in the study area of the Šibenik channel. Reflection ( $R_w$ ) of VIS bands: B1—coastal aerosol, B2—blue, B3—green, B4—red were compared to the MB soundings.

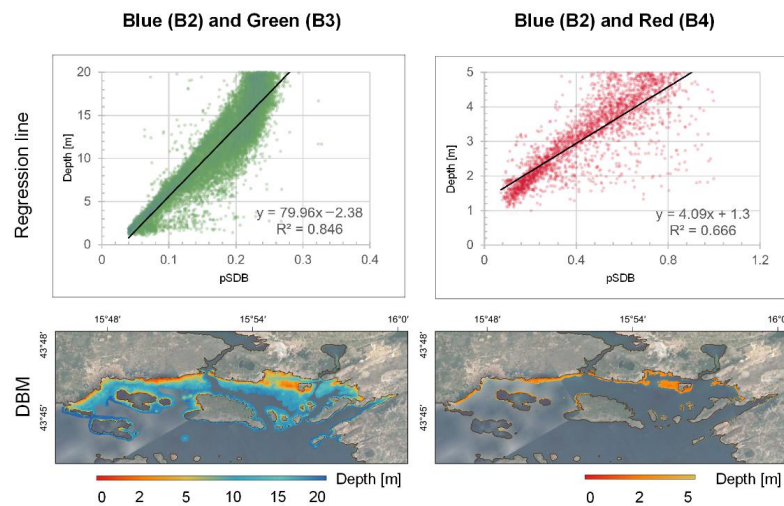


**Figure 9.** G SDB and R SDB in a coastal area of the Šibenik channel (middle Adriatic) extracted from the optimal Sentinel-2 MSI acquired on 30 September 2017 using the log band ratio method. The SDB models were estimated by vertical referencing the pseudo depth,  $\ln(\text{blue})/\ln(\text{green})$  and  $\ln(\text{blue})/\ln(\text{red})$  to the mean low lower water (MLLW) using in situ MB soundings.

**Table 7.** Depth range and quality of green (G) SDB and red (R) SDB.

	SDB G Blue (B2) and Green (B3)	SDB R Blue (B2) and Red (B4)
Depth range [m]	0–20	0–5
RMSE [m]	2.14	0.66
MedAE [m]	1.23	0.45

A switch model (Figure 10) combining R SDB and G SDB was calculated using the weighted mean under the following conditions [40]:

$$= \begin{cases} \text{SDB R} & \text{za SDB R} < 3 \\ \text{SDB G} & \text{za SDB R} > 3 \text{ i SDB G} > 5 \\ \alpha\text{SDB G} + \beta\text{SDB R} & \text{za SDB R} \geq 3 \text{ i SDB G} \leq 5 \end{cases} \quad (7)$$

where:

$$\alpha = \frac{5 - \text{SDB R}}{3}; \beta = 1 - \alpha \quad (8)$$

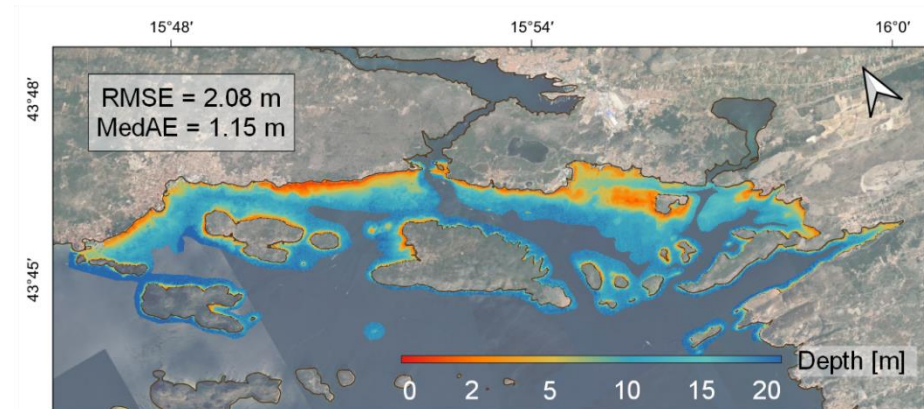


**Figure 10.** Switch SDB model of the Šibenik channel covering depth range 0–20 m estimated from the Sentinel-2 image acquired on 30 September 2017 using the LBR algorithm with band combinations with blue, green, and red bands.

As predicted models (G, R, and Switch) cover different depth ranges, the NMedAE was calculated for the overlapping depth ranges (Figure 11). Compared to G SDB, R SDB was a better solution, more sensitive to depth change, in the marine area shallower than 5 m (a few times smaller NMedAE). In the depth range from 5 m to 20 m, the G SDB model showed great alignment with in situ MB data (NMedAE = 10%). The combination of the two SDB models resulted in the enhanced switch model that had better performance in the shallow area (depth < 5 m) while preserving the depth quality of the G SDB in the depth range 5–20 m.

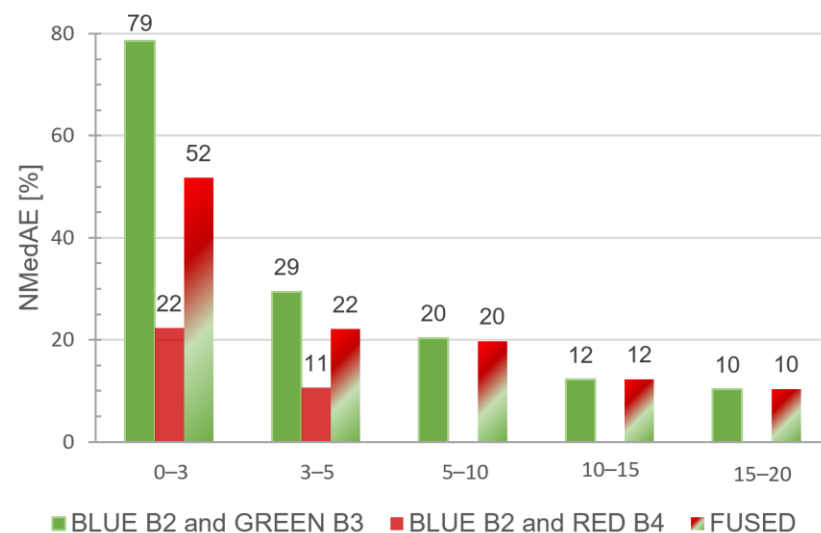


**Figure 11.** Normalized median absolute error for G SDB (B2 and B3), R SDB (B2 and B4), and switch SDB in different depth ranges.

#### 4. Discussion and Conclusions

The radiance measured by the satellite sensor over sea areas is a product of signal interaction with the atmosphere and water system. Up to 90 percent of the radiance registered by the satellite sensor is a product of the signal's two-way path through the atmosphere [13]. For this reason, the top-of-atmosphere reflectance must be reduced to the

water's leaving reflectance. The other task for the AC processor, apart from modelling the atmospheric path of the signal, is to remove the "noise" including sun glint or adjacency effects. AC processors are developed for different sensors, water types, and sun angles, using different algorithms with optional additional filters. In this study, five different AC processors, namely: Sen2Cor, Acolite, C2RCC, and iCOR were compared. Their performance for bathymetry retrieval using an empirical approach [34] from Sentinel-2 MSI was assessed in the middle Adriatic. The main difference between the AC processors is in a model or a method to estimate the scattering from the atmosphere, especially the irregular and accidental Mie (aerosol) scattering. Another difference is the possibility of eliminating the reflectance from surfaces (sea surface, adjacent land, and vegetation) or reflection from dissolved material in the water column (turbidity). Their performance in retrieving BOA reflection for further bathymetry modelling is conditioned by the methods each AC processor performs. Consequently, each AC processor has pros and cons. Sen2Cor is used by ESA to distribute the Sentinel-2 L2A MSI (BOA) from Sentinel-2 L1A MSI (TOA) through Copernicus Open Access Hub. It applies the DDV algorithm [48] to model the AOT and it is intended to use over land. The product of Sen2Cor, Sentinel-2 MSI L2A, is frequently used for SDB modelling e.g., [24,36]

However, the results in this study demonstrate that Acolite DSF, Acolite EXP, C2RCC, or iCOR applied to the Sentinel-2 L1C MSI outperformed the Sentinel-2 L2A MSI (Sen2Cor) regarding the depth estimation. AC processors derive different BOA reflectance from the same L1C MSI scene due to different models of AOT modelling and extra modules to eliminate radiance different from one reflected from the bottom of the sea. Acolite EXP processor assumes that after the correction for Rayleigh scattering, the SWIR band contains only information about reflectance scattered from aerosols and extrapolates the SWIR to VIS bands by exponential function [29]. However, MSI in the coastal marine area is influenced by the reflectance from the sea surface, commonly sunglint, and reflectance from the surrounding land area. This leads to the underestimation of Rrs in VIS bands. Acolite DSF with automatic choice of the band with the lowest value of atmospheric path overcomes this issue [29]. C2RCC was designed for turbid waters [31] and when applied to a low-turbid marine area such as the middle Adriatic, it produced the lowest correlation, and more robust SDB products with lower accuracy than other AC processors. However, C2RCC outperformed other AC algorithms when scenes suffered a severe sunglint or adjacency effect. iCOR has a specific module SIMEC [33], designed to reduce the radiation scattered from the adjacent land or vegetation. This module was designed to improve the performance of AC processor over marine areas. When applied to Sentinel-2 MSI, the overall performance in bathymetry retrieval was satisfactory. However, a few scenes were incorrectly masked ( $2 \times 2$  km gaps) because of SIMEC correction.

The results of scene-by-scene analyses depicted the two groups of AC correction algorithms. Acolite DSF, Acolite EXP, and iCOR in the first group produced a greater correlation with MB soundings with smaller depth uncertainty. Sen2Cor and C2RCC in the second group had coarser results. Acolite EXP masked out the shallowest, coastal marine areas due to sun glint or adjacency effects, and iCOR correction produced large masked areas ( $2 \times 2$  km) on several images that would create gaps in the final SDB bathymetry model. Accordingly, Acolite DSF was selected as an optimal AC processor for the area.

The selection of spectral bands for bathymetry estimation depends upon the sensor, the absorption coefficient of the spectral band in water, and the conditions of the water column [57]. The atmosphere is opaque for the ultraviolet (UV) part of the EM spectrum [13] and water absorbs almost all infrared (IR) radiance. The seafloor in shallow areas can be reached by the VIS part of the EM spectrum with a range of wavelength from 380 nm to 700 nm. Theoretically, smaller absorption coefficients in water have spectral bands with smaller wavelengths [53]. The log band ratio algorithm suggested by Stumpf et al. [34] uses the combination of blue (445 nm–515 nm) and green (510 nm–595 nm) VIS bands. However, it can be utilized with other band combinations. Red or yellow spectral bands are successful in retrieving bathymetry in turbid areas [57] or areas with low bottom albedo. In addition,

red bands register the depth gradient in the narrow coastal areas (usually up to 5 m deep) more precisely than green or blue bands [39,57,58]. Recently, the coastal blue band has been applied in bathymetry mapping using the high-resolution MSI [58,59]. Sentinel-2 MSI has four bands in the VIS part of the spectrum: B1—coastal aerosol, B2—blue, B3—green, and B4—red. As compared to the other VIS bands of Sentinel-2 MSI, band 1—Coastal (blue) aerosol—has a larger signal-to-noise ratio and the lowest spatial resolution. For that reason, it was excluded from bathymetry modelling. This study adopted the weighted mean between SDB derived from the LBR algorithm using different combinations of spectral bands [40]. The log band ratio with the red part of the spectrum enhanced the coastal bathymetry up to 5 m deep, where the classic green combination [34] had a normalized median absolute error of over 80%.

With large gaps between in situ surveys or outdated bathymetry data in coastal areas, there is an urgent demand for effective and low-cost technology able to deliver reliable data. Although the accuracy of the SDB is still not comparable to the classic bathymetric techniques, this research demonstrated it can be improved by the choice of AC processor and optimal spectral bands.

**Author Contributions:** Conceptualization, L.V. and J.K.P.; methodology, L.V. and J.K.P.; software, L.V. and J.K.P.; validation, L.V. and J.K.P.; formal analysis, L.V. and J.K.P.; investigation, L.V. and J.K.P.; resources, L.V. and J.K.P.; data curation, L.V. and J.K.P.; writing—original draft preparation, L.V. and J.K.P.; writing—review and editing, L.V. and J.K.P.; visualization, L.V. and J.K.P.; supervision, L.V. and J.K.P.; project administration, L.V. and J.K.P.; funding acquisition, L.V. and J.K.P. All authors have read and agreed to the published version of the manuscript.

**Funding:** This research is partially supported through project KK.01.1.1.02.0027, a project co-financed by the Croatian Government and the European Union through the European Regional Development Fund—the Competitiveness and Cohesion Operational Programme.

**Data Availability Statement:** Sentinel-2 multispectral images used in study were downloaded from Copernicus Open Access Hub. Bathymetric data is available by negotiation from Hydrographic Institute of the Republic of Croatia.

**Acknowledgments:** The authors would like to thank the Hydrographic Institute of the Republic of Croatia for kindly providing the bathymetric data sets for the research.

**Conflicts of Interest:** The authors declare no conflict of interest.

## References

1. IMO—International Maritime Organization. International Convention for the Safety of Life at Sea. Available online: <https://www.refworld.org/docid/46920bf32.html> (accessed on 29 January 2022).
2. International Hydrographic Organization (IHO). Publication M-2: The Need for National Hydrographic Services, IHO, Monaco, 2018. Available online: [https://iho.int/iho\\_pubs/misc/M-2\\_3.0.7\\_E\\_06142018.pdf](https://iho.int/iho_pubs/misc/M-2_3.0.7_E_06142018.pdf) (accessed on 20 October 2022).
3. Makowski, C.; Finkl, C.W. *Seafloor Mapping along Continental Shelves: Research and Techniques for Visualizing Benthic Environments*; Springer: Cham, Switzerland, 2016.
4. UN Environment Programme. Coastal Zone Management. Available online: <https://www.unep.org/explore-topics/oceans-seas/what-we-do/working-regional-seas/coastal-zone-management> (accessed on 29 January 2022).
5. Lichter, M.; Vafeidis, A.T.; Nicholls, R.J.; Kaiser, G. Exploring Data-Related Uncertainties in Analyses of Land Area and Population in the “Low-Elevation Coastal Zone” (LECZ). *J. Coast. Res.* **2011**, *27*, 757–768. [CrossRef]
6. Nicholls, R.J.; Cazenave, A. Sea-Level Rise and Its Impact on Coastal Zones. *Science* **2010**, *328*, 1517–1520. [CrossRef] [PubMed]
7. Vilibić, I.; Denamiel, C.; Zemunik, P.; Monserrat, S. The Mediterranean and Black Sea meteotsunamis: An overview. *Nat. Hazards* **2021**, *106*, 1223–1267. [CrossRef]
8. International Hydrographic Organization (IHO). Publication C-55: Status of Hydrographic Surveying and Charting Worldwide. IHO, Monaco, 2022. Available online: <https://iho.int/uploads/user/pubs/cb/c-55/c55.pdf> (accessed on 29 January 2022).
9. International Hydrographic Organization (IHO). Standard S-44: IHO Standards for Hydrographic Surveys. IHO, Monaco, 2020. Available online: [https://iho.int/uploads/user/pubs/standards/s-44/S-44\\_Edition\\_6.0.0\\_EN.pdf](https://iho.int/uploads/user/pubs/standards/s-44/S-44_Edition_6.0.0_EN.pdf) (accessed on 29 January 2022).
10. De Jong, C.D.; Lachapelle, G.; Skone, S.; Elema, I.A. *Hydrography*; VSSD: Delft, The Netherlands, 2012.
11. Irish, J.L.; White, T.E. Coastal engineering applications of high-resolution lidar bathymetry. *Coast. Eng.* **1997**, *35*, 47–71. [CrossRef]
12. Argans. Sentinel Coastal Charting Worldwide—Final Report. 2019. Available online: <https://eo4society.esa.int/wp-content/uploads/2020/01/FinalReportCoastalCharting.pdf> (accessed on 20 October 2022).

13. Robinson, I.S. *Discovering the Ocean from Space: The Unique Applications of Satellite Oceanography*; Springer/Praxis Publishing: Berlin, Germany, 2010.
14. European Space Agency. Sen2Cor Configuration and User Manual. 2021. Available online: <http://step.esa.int/thirdparties/sen2cor/2.10.0/docs/S2-PDGS-MPC-L2A-SUM-V2.10.0.pdf> (accessed on 20 October 2022).
15. Copernicus Open Access Hub. Available online: <https://scihub.copernicus.eu/> (accessed on 30 January 2022).
16. Casal, G.; Monteys, X.; Hedley, J.; Harris, P.; Cahalane, C.; McCarthy, T. Assessment of empirical algorithms for bathymetry extraction using Sentinel-2 data. *Int. J. Remote Sens.* **2019**, *40*, 1–25. [[CrossRef](#)]
17. Caballero, I.; Stumpf, R. Atmospheric correction for satellite-derived bathymetry in the Caribbean waters: From a single image to multi-temporal approaches using Sentinel-2A/B. *Optics Express* **2020**, *28*, 11742–11766. [[CrossRef](#)]
18. Renosh, P.R.; Doxaran, D.; Keukelaere, L.D.; Gossn, J.I. Evaluation of Atmospheric Correction Algorithms for Sentinel-2-MSI and Sentinel-3-OLCI in Highly Turbid Estuarine Waters. *Remote Sens.* **2020**, *12*, 1285. [[CrossRef](#)]
19. Duan, Z.; Chu, S.; Cheng, L.; Ji, C.; Li, M.; Shen, W. Satellite-derived bathymetry from Landsat-8 and Sentinel-2A images: Assessment of atmospheric correction and depth derivation models for shallow waters. *Opt. Express* **2022**, *30*, 3238–3261. [[CrossRef](#)]
20. Vrdoljak, L.J.; Režić, M.; Petričević, I. Bathymetric and geological properties of the Adriatic Sea. *Rud. -Geološko Naft. Zb.* **2021**, *36*, 2. [[CrossRef](#)]
21. GeoAdriatic-Official Hydrographic Survey Browser. Available online: <https://geoadriatic.hhi.hr/en/> (accessed on 20 October 2022).
22. CDI Data Discovery and Access Service—EMODnet Bathymetry. Available online: <https://www.emodnet-bathymetry.eu/search> (accessed on 20 October 2022).
23. Morović, M.; Grbec, B.; Matić, F.; Bone, M.; Matijević, S. Optical Characterization of the Eastern Adriatic Waters. *Fresenius Environ. Bull.* **2008**, *17*, 1679–1687.
24. Leder, N.; Duplančić Leder, T. Optimal Conditions for Satellite Derived Bathymetry (SDB)—Case Study of the Adriatic Sea. In Proceedings of the FIG Working Week, Amsterdam, The Netherlands, 10–14 May 2020.
25. Sextant Catalogue Service—Satellite Derived Bathymetry Central Dalmatia—Croatia. Available online: [https://www.emodnet-bathymetry.eu/metadata-amp-data/composite-dtms-catalogue-service#/metadata/SDN\\_CPRD\\_4667\\_croatia2004](https://www.emodnet-bathymetry.eu/metadata-amp-data/composite-dtms-catalogue-service#/metadata/SDN_CPRD_4667_croatia2004) (accessed on 20 October 2022).
26. Vanhellemont, Q.; Ruddick, K. Atmospheric correction of metre-scale optical satellite data for inland and coastal water applications. *Remote Sens. Environ.* **2018**, *216*, 586–597. [[CrossRef](#)]
27. Vanhellemont, Q.; Ruddick, K. Atmospheric correction of Sentinel-3/OLCI data for mapping of suspended particulate matter and chlorophyll-a concentration in Belgian turbid coastal waters. *Remote Sens. Environ.* **2021**, *256*, 112284. [[CrossRef](#)]
28. Vanhellemont, Q. Adaptation of the dark spectrum fitting atmospheric correction for aquatic applications of the Landsat and Sentinel-2 archives. *Remote Sens. Environ.* **2019**, *225*, 175–192. [[CrossRef](#)]
29. Vanhellemont, Q.; Ruddick, K. ACOLITE For Sentinel-2: Aquatic Applications of MSI imagery. In Proceedings of the 2016 ESA Living Planet Symposium, Prague, Czech Republic, 9–13 May 2016; ESA Special Publication SP-740: Noordwijk, The Netherlands, 2016; pp. 9–13.
30. Doerffer, R.; Schiller, H. The MERIS case 2 water algorithm. *Int. J. Remote Sens.* **2007**, *28*, 517–535. [[CrossRef](#)]
31. Brockmann, C.; Doerffer, R.; Peters, M.; Stelzer, K.; Embacher, S.; Ruescas, A. Evolution of the C2RCC Neural Network for Sentinel 2 and 3 for the Retrieval of Ocean Colour Products in Normal and Extreme Optically Complex Waters. In Proceedings of the Living Planet Symposium, Prague, Czech Republic, 9–13 May 2016.
32. Sterckx, S.; Knaeps, E.; Adriaensen, S.; Reusen, I.; De Keukelaere, L.; Hunter, P. Opera: An Atmospheric Correction for Land and Water. In Proceedings of the ESA Sentinel-3 for Science Workshop, Venice, Italy, 2–5 June 2015.
33. Sterckx, S.; Knaeps, S.; Kratzer, S.; Ruddick, K. SIMilarity Environment Correction (SIMEC) applied to MERIS data over inland and coastal waters. *Remote Sens. Environ.* **2014**, *157*, 96–110. [[CrossRef](#)]
34. Stumpf, R.P.; Holderied, K.; Sinclai, M. Determination of Water Depth with High-Resolution Satellite Imagery over Variable Bottom Types. *Limnol. Oceanogr.* **2003**, *48*, 547–556. [[CrossRef](#)]
35. Evagorou, E.; Mettas, C.; Agapiou, A.; Themistocleous, K.; Hadjimitsis, D. Bathymetric maps from multi-temporal analysis of Sentinel-2 data: The case study of Limassol, Cyprus. *Adv. Geosci.* **2019**, *45*, 397–407. [[CrossRef](#)]
36. Duplančić Leder, T.; Leder, N.; Peroš, J. Satellite Derived Bathymetry Survey Method-Example of Hramina Bay. *Trans. Marit. Sci.* **2019**, *8*, 99–108. [[CrossRef](#)]
37. Traganos, D.; Poursanidis, D.; Aggarwal, B.; Chrysoulakis, N.; Reinartz, P. Estimating Satellite-Derived Bathymetry (SDB) with the Google Earth Engine and Sentinel-2. *Remote Sens.* **2018**, *10*, 859. [[CrossRef](#)]
38. Westley, K. Satellite Derived Bathymetry for maritime archeology: Testing its effectiveness at two ancient harbours in the Eastern Mediterranean. *J. Archaeol. Sci. Rep.* **2021**, *38*, 103030.
39. Caballero, I.; Stumpf, R. Retrieval of nearshore bathymetry from Sentinel-2A and 2B satellites in South Florida coastal waters. *Estuar. Coast. Shelf Sci.* **2019**, *226*, 106277. [[CrossRef](#)]
40. Caballero, I.; Stumpf, R.P. Towards Routine Mapping of Shallow Bathymetry in Environments with Variable Turbidity: Contribution of Sentinel-2A/B Satellites Mission. *Remote Sens.* **2020**, *12*, 451. [[CrossRef](#)]
41. Muzirafuti, A.; Barreca, G.; Crupi, A.; Faina, G.; Paltrinieri, D.; Lanza, S.; Randazzo, G. The Contribution of Multispectral Satellite Image to Shallow Water Bathymetry Mapping on the Coast of Misano Adriatico, Italy. *J. Mar. Sci. Eng.* **2020**, *8*, 126. [[CrossRef](#)]

42. Lamb, D.; Verlinde, J. *Physics and Chemistry of Clouds*; Cambridge University Press: Cambridge, UK, 2011.
43. Platt, U.; Pfeilsticker, K.; Vollmer, M. *Radiation and Optics in the Atmosphere*; Springer: New York, NY, USA, 2007.
44. Hedley, J.; Harborne, A.; Mumby, P. Technical note: Simple and robust removal of sun glint for mapping shallow-water benthos. *Int. J. Remote Sens.* **2005**, *26*, 2107–2112. [[CrossRef](#)]
45. Liang, S.; Xiaowen, L.; Wang, J. *Advanced Remote Sensing*; Academic Press: Cambridge, MA, USA, 2012.
46. Main-Knorn, M.; Pflug, B.; Louis, J.; Debaecker, V.; Müller-Wilm, U.; Gascon, F. Sen2Cor for Sentinel-2. In Proceedings of the Conference: Image and Signal Processing for Remote Sensing, Warsaw, Poland, 11–13 September 2017.
47. Richter, R. A fast atmospheric correction algorithm applied to Landsat TM images. *Remote Sens.* **1990**, *11*, 159–166. [[CrossRef](#)]
48. Kaufman, Y.J.; Sendra, C. Algorithm for automatic atmospheric corrections to visible and near-IR satellite imagery. *Int. J. Remote Sens.* **1988**, *9*, 1357–1381. [[CrossRef](#)]
49. Royal Belgian Institute of Natural Sciences: Operational Directorate Natural Environment-Scientific Web Sites and Applications. Available online: <https://odnature.naturalsciences.be/remsem/software-and-data/acolite> (accessed on 7 February 2022).
50. Pahlevan, N.; Sarkar, S.; Franz, B.A.; Balasubramanian, S.V.; He, J. Sentinel-2 MultiSpectral (MSI) data processing for aquatic science applications: Demonstration and validations. *Remote Sens. Environ.* **2017**, *201*, 47–56. [[CrossRef](#)]
51. Guanter, L. New Algorithms for Atmospheric Correction and Retrieval of Biophysical Parameters in Earth Observation. Application to ENVISAT/MERIS Data. Doctoral Thesis, University of Valencia, Valencia, Spain, 2007.
52. Pe’eri, S.; Parrish, C.; Azuike, C.; Lee, A.; Armstrong, A. Satellite Remote Sensing as a Reconnaissance Tool for Assessing Nautical Chart Adequacy and Completeness. *Mar. Geod.* **2014**, *37*, 293–314. [[CrossRef](#)]
53. Pope, R.M.; Fry, E.S. Absorption spectrum (380–700 nm) of pure water. II. Integrating cavity measurements. *Appl. Opt.* **1997**, *36*, 8710–8723. [[CrossRef](#)]
54. European Marine Observation and Data Network: EMODnet Geology. Available online: <https://www.emodnet-geology.eu/> (accessed on 10 December 2021).
55. European Space Agency ESA. Sentinel-2 User Handbook, 2015. Available online: [https://sentinels.copernicus.eu/web/sentinel/user-guides/document-library/-/asset\\_publisher/xslst4309D5h/content/sentinel-2-user-handbook](https://sentinels.copernicus.eu/web/sentinel/user-guides/document-library/-/asset_publisher/xslst4309D5h/content/sentinel-2-user-handbook) (accessed on 31 January 2022).
56. The European Space Agency ESA. Data Products. Available online: <https://sentinel.esa.int/web/sentinel/missions/sentinel-2/data-products> (accessed on 7 February 2022).
57. Gao, J. Bathymetric mapping by means of remote sensing: Methods, accuracy, and limitations. *Prog. Phys. Geogr. Earth Environ.* **2009**, *33*, 103–116. [[CrossRef](#)]
58. Bramante, J.F.; Raju, D.K.; Sin, T.M. Multispectral Derivation of Bathymetry in Singapore’s Shallow, Turbid Waters. *Int. J. Remote Sens.* **2013**, *34*, 2070–2088. [[CrossRef](#)]
59. Poppenga, S.K.; Palaseanu-Lovejoy, M.; Gesch, D.B.; Danielson, J.J.; Tyler, D.J. Evaluating the potential for near-shore bathymetry on the Majuro Atoll, Republic of the Marshall Islands, using Landsat 8 and WorldView-3 imagery. *U.S. Geol. Surv. Sci. Investig. Rep.* **2018**, *5024*, 14.